Natural isotopic abundance ^{13}C and ^{15}N multidimensional solid-state NMR enabled by dynamic nuclear polarization

Adam Smith, Katharina Märker, Sabine Hediger, Gaël de Paëpe

Natural Isotopic Abundance ^{13}C and ^{15}N Multidimensional Solid-State NMR Enabled by Dynamic Nuclear Polarization

*Adam N. Smith[1], Katharina Märker[1,2], Sabine Hediger[1], Gaël De Paëpe[1]**

[1]Univ. Grenoble Alpes, CEA, CNRS, INAC, MEM, F-38000 Grenoble, France, [2] Present address: Department of Chemistry, University of Cambridge, Lensfield Road, Cambridge CB2 1EW, United Kingdom.

Corresponding Author

*Gaël De Paëpe: gael.depaepe@cea.fr.

ABSTRACT Dynamic nuclear polarization (DNP) has made feasible solid-state NMR experiments that were previously thought impractical due to sensitivity limitations. One such class of experiments is the structural characterization of organic and biological samples at natural isotopic abundance (NA). Herein, we describe the many advantages of DNP-enabled ssNMR at NA, including the extraction of long-range distance constraints using dipolar recoupling pulse sequences without the deleterious effects of dipolar truncation. In addition to the theoretical underpinnings in the analysis of these types of experiments, numerous applications of DNP-enabled ssNMR at NA are discussed.

TOC GRAPHICS

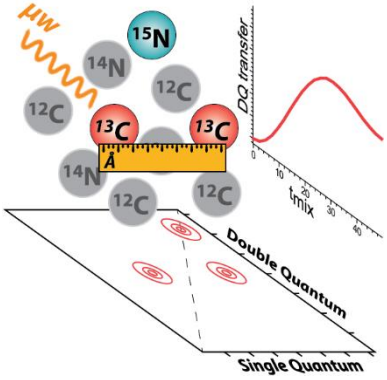

KEYWORDS Magic angle spinning, Dynamic Nuclear Polarization, dipolar recoupling, sensitivity enhancement, correlation experiment, dipolar truncation

The determination of molecular structure is essential to understand function. This canon is central to an array of fields, ranging from materials chemistry to structural biology. Over the years, magic angle spinning solid state NMR (MAS ssNMR) has proved invaluable in obtaining structural information with atomic resolution. A particular strength of the technique is that long-range order within the sample is not required (i.e. *sans* crystallization). As a result, heterogeneous molecular assemblies, such as amyloid fibrils, membrane proteins, heterogeneous catalysts, polymorphic pharmaceuticals, etc. are amenable to high-resolution structural studies by MAS ssNMR.[1–4]

Despite the rich information content yielded from MAS ssNMR, the technique suffers from poor sensitivity. This lack of sensitivity is due to the small population difference between nuclear spin states at available magnetic field strengths. For example, only ~ 0.02 % of ^{1}H nuclei are polarized at 100 K and 23.5 T. The latter is considered under an ideal scenario, that is the polarization of a high gyromagnetic ratio nucleus (γ_{1H} = 42.6 MHz/ T), at the highest commercially available NMR magnetic field (^{1}H resonant frequency = 1 GHz), and at cryogenic temperatures (100 K). Over the years, many advances in NMR were made to combat low sensitivity, including cryogenically cooled probes and preamplifiers,[5] efficient isotopic enrichment schemes,[6–10] pulse sequence development,[11] and high magnetic field technology.[12,13] In addition, over the last two decades there has been a sensitivity revolution in solid-state NMR, namely the development of magic angle spinning dynamic nuclear polarization (MAS-DNP).[14,15] In MAS-DNP experiments, the relatively larger polarization of electron spins in paramagnetic dopants is transferred to NMR active nuclei resulting in sensitivity gains that can yield several orders of magnitude in experimental time savings.[16,17]

The substantial gain in sensitivity afforded by DNP has opened new experimental avenues in MAS ssNMR, for example, structural studies of proteins and materials at natural isotopic abundance (NA). Herein, we will discuss the advantages of MAS ssNMR experiments performed at NA and enabled by DNP, focusing on bio-organic applications that involve the detection of ^{1}H, ^{13}C, and ^{15}N nuclei, and their use in structural measurements. Impressive results have also been obtained on other types of systems, involving the detection of low gamma nuclei at NA (e.g. ^{17}O, ^{43}Ca, ^{89}Y, etc.),[18–21] however, these studies are beyond the scope of this review.

1 - Motivation for NA ssNMR studies

The NA of NMR active nuclei varies largely throughout the periodic table. For example, ^{1}H is 99.9 % abundant, whereas ^{13}C is only 1.1 % abundant. Table 1 lists the isotopic abundance for some of the more commonly observed NMR active nuclei, in addition the receptivity factor, a measure of how sensitive a particular nucleus is relative to ^{1}H is given. The high NA and large gyromagnetic ratio of ^{1}H (γ_{1H} = 42.6 MHz/ T) makes it a logical (and popular) choice for NMR studies. However, in ssNMR, where anisotropic interactions such as dipolar couplings are not averaged by molecular tumbling, ^{1}H-detected NMR experiments can be problematic because of poor spectral resolution (resulting from the presence of large ^{1}H-^{1}H dipolar couplings). In contrast, heteronuclei (e.g. ^{13}C, ^{15}N, etc.) usually provide improved resolution thanks to larger spectral dispersion and narrower linewidths that can be obtained using efficient ^{1}H decoupling combined with MAS.

Table 1. Natural isotopic abundance of commonly observed NMR active nuclei.

Isotope	Abundance (%)	Nuclear spin (I)	γ (MHz/ T)	Receptivity relative to ^{1}H [a]
^{1}H	99.985	1/2	42.58	1.0
^{2}H	0.015	1	6.54	1.5×10^{-6}

^{13}C	1.108	1/2	10.71	1.7×10^{-4}
^{15}N	0.365	1/2	-4.32	3.8×10^{-6}
^{17}O	0.037	5/2	-5.77	1.1×10^{-5}
^{29}Si	4.683	1/2	-8.47	3.7×10^{-4}

[a] $R^X = NA \times |\gamma^3| \times I(I+1)/R^{1H}$

To take advantage of the favorable characteristics of these heteronuclei with ssNMR, it is typically necessary to enrich the sample with the isotope of interest for the requisite sensitivity to perform advanced ssNMR experiments, such as recording multidimensional correlation spectra. In fact, for many biomolecular systems, it has become relatively straightforward to isotopically enrich samples with ^{13}C, ^{15}N, and ^{2}H, both uniformly and sparsely with modern molecular biology techniques.[6–9] However, for systems that are not amenable to those techniques, it is oftentimes cost prohibitive for isotopic enrichment due to the complex synthetic schemes used in their production, which makes it imperative to study such samples at their NA.

Also, in both material and biomolecular systems, the environment can influence the structural and functional characteristics of the sample. For example, the cellular milieu is composed of a complex mixture of small molecules, organelles, and proteins, all of which can have a dramatic influence on the structure of biomolecules. In addition, *in-situ* and *operando* studies of materials are becoming increasingly important in the development of catalysts, active pharmaceutical ingredients (APIs), functional polymers, carbohydrate-based materials, biomass treatment, batteries, etc. Therefore, there is a need to characterize these samples in, or derived from, their native environment. This frequently excludes isotopic enrichment protocols, necessitating the study of samples at NA.

Apart from the lower cost, higher availability, and relevance of NA samples, another exciting advantage of their use lies in the greatly simplified spin dynamics in dilute spin systems. For

example, the observation and measurement of long-range distances (> 3 Å) is greatly facilitated as most spin pairs of interest are isolated. This means that MAS ssNMR experiments at NA can be advantageous, even when facile isotopic enrichment of samples is possible. This aspect of NA experiments will be explained in more detail in the following sections.

2 - Overcoming the sensitivity challenges of NA ssNMR by DNP

The low NA of NMR active nuclei presents a significant challenge with respect to experimental sensitivity, which can however be overcome by using MAS-DNP. Below, a brief description on MAS-DNP transfer mechanisms and the practical considerations of MAS-DNP experiments is given.

An unpaired electron has a gyromagnetic ratio of ~ 28 GHz/ T, leading to a larger population difference (or polarization) between spin states compared to NMR active nuclei ($\gamma_e/\ \gamma_{1H} \approx 660$). In DNP experiments, the aim is to transfer the larger polarization of an unpaired electron to nuclei resulting in a drastic increase in sensitivity.[22,23] To date, the most efficient DNP transfer mechanism, at high-fields (≥ 5 T) and under MAS, is the cross-effect (CE).[24] The CE occurs in a three-spin system of two electrons and one nucleus. The two electron spins are coupled by dipolar and exchange interactions, and inhomogenously broadened by a large *g*-anisotropy. The nucleus interacts with the electrons via hyperfine couplings. The energy levels from the resulting spin system are modulated by MAS and result in three distinct "rotor events" that mediate the generation of hyperpolarization of nuclei.[25–28] The first type of "rotor event" occurs when the resonant condition $\omega_{\mu w} = \omega_{e1}$ (or ω_{e2}) is met and generates a large polarization difference between the two coupled electrons, where $\omega_{\mu w}$ is the microwave irradiation frequency and ω_e is an electron Larmor frequency. The second type of "rotor event" occurs when the CE condition $|\omega_{e1} - \omega_{e2}| = \omega_n$ is met, where ω_n is the nuclear Larmor frequency, yielding a transfer of the electron polarization

difference to the nucleus. The third type of "rotor event" occurs when $\omega_{e1} = \omega_{e2}$, termed a "dipolar event", and results in an exchange of electron polarization which should maintain the polarization difference between the two electrons to enable the buildup of nuclear hyperpolarization through successive CE events. Hyperpolarization is transferred from the hyperfine coupled nucleus to the bulk nuclei by nuclear spin diffusion.

In addition to the theoretical underpinnings of MAS-DNP transfer mechanisms, specialized instrumentation and sample preparation are required for efficient MAS-DNP to occur. The source of unpaired electrons - the polarizing agent - and its introduction into the sample is critical in MAS-DNP experiments. In general, suitable CE polarization agents consist of two radicals tethered together to form a biradical.[29] The use of biradicals ensures that the two unpaired electrons are strongly coupled by dipolar and exchange interactions.[30,31] Oftentimes, the linker moiety is tuned to optimize these interactions. In addition, the linker can be functionalized to generate desired chemical properties (e.g. hydrophilicity) of the polarization agent or to target it to specific parts of a sample.[32–40] The polarization agent has to be homogeneously distributed in the sample to achieve efficient MAS-DNP. It is thus typically dissolved in a glass-forming mixture (containing glycerol or DMSO for instance) that can be used to suspend or impregnate the sample of interest.[15,41] Removal of the excess matrix can also be envisioned, where appropriate, either with the Matrix Free or Film Casting sample preparation approaches, as long as radical aggregation is avoided.[36,42,43]

The instrumentation requirements for MAS-DNP are numerous, the primary components of a MAS-DNP system being a ssNMR magnet and spectrometer, a microwave source, and a cooling system coupled to a cryogenic MAS probe. To date, commercial MAS-DNP instrumentation is available at magnetic fields of 9.4, 14.1, 18.8, and 21.1 T.[44] The corresponding electron resonant

frequencies (for a $g \approx 2$ electron) for the latter magnetic fields are 263, 395, 527, and 591 GHz. Currently, gyrotrons are the most utilized microwave sources capable of providing the required high-frequency microwave irradiation with sufficient power for CE MAS-DNP. Also, for favorable electron relaxation rates CE MAS-DNP is conducted at cryogenic temperatures. The sample is actively cooled and rotated at ~ 100 K with commercial MAS-DNP instrumentation.[44–46] This is achieved by passing the N_2 gas used to cool and spin the sample through pressurized heat exchangers that are submerged in liquid N_2.

3 – MAS-DNP-assisted NMR crystallography

Structural studies of organic solids which are not suitable for single crystal X-ray diffraction can greatly profit from ssNMR. "NMR crystallography" studies have relied strongly on ^{1}H NMR (e.g. ^{1}H-X HETCOR spectra) and the comparison of experimental chemical shifts to those calculated by density functional theory (DFT) or other computational methods.[47–49] Through this comparison chemical structures can be validated from a given set of models. In general, ^{1}H-X HETCOR experiments are used because of the high sensitivity of ^{1}H compared to the lower-γ X nucleus. From these experiments the chemical shifts of X-, and if resolution permits, ^{1}H-nuclei are measured for comparison to those calculated from candidate structures. In cases where greater spectral dispersion is required for the assignment of resonances ^{13}C-^{13}C correlation spectra can be acquired using INADEQUATE-type experiments.[50,51] These methods have been successfully used for structure determination on numerous systems and this type of approach has been expedited when used in combination with MAS-DNP techniques.[47,48,52,53]

Probing polymorphism using chemical shifts

Structural polymorphs occur in many solid-state systems and often have a dramatic impact on the function and properties of the material. Therefore, it is critical to be able to differentiate and

characterize the different polymorphs within a given system. Chemical shifts report on the environment of their respective nuclei and are therefore particularly adept at characterizing structural polymorphs. APIs (active pharmaceutical ingredients) are a class of molecules that can have numerous polymorphic conformations, and it is necessary to characterize them before the pharmaceutical can be employed. In addition, the API is often diluted in excipients, this dilution makes them extremely difficult to characterize *in-situ* by conventional MAS ssNMR approaches, however, the added sensitivity of MAS-DNP enables *in-situ* studies of APIs at NA.[54] In one example, Ni Q.Z. *et al.* were able to obtain ^{1}H-^{13}C and ^{1}H-^{15}N correlations of the API posaconazole in amorphous solid dispersions of vinyl acetate.[55] Interestingly, in this study the MAS-DNP polarization agent was incorporated with the sample using spray drying or hot-melt extrusion, both of which are techniques to produce amorphous solid dispersions in the pharmaceutical industry. In a separate study by Pinon A.C. *et al*. of the API theophylline, MAS-DNP was used to characterize three polymorphs of the drug. In addition, they observed polymorphic transitions of the API that were induced by addition of the polarization agent by impregnation.[56] However, they were able to devise alternative sample preparation techniques, such as grinding under an inert atmosphere, which prevented these induced polymorphic phase transitions.

DFT-free resonance assignment

With the limited ^{1}H resolution in ssNMR, ambiguities in the assignment of ^{1}H, ^{13}C, and ^{15}N resonances can easily occur in the approaches described above. Their assignment therefore necessarily relies on the comparison between experimentally measured chemical shifts and those computed from candidate structures. However, Märker et al. showed that even moderate ($\varepsilon_{on/off}$ = 11) MAS-DNP enhancements are sufficient to record 2D ^{13}C-^{13}C and ^{13}C-^{15}N correlation spectra of a self-assembled deoxyguanosine derivative at NA.[57] This enabled the full assignment of ^{13}C

and ^{15}N resonances, which was not possible from proton-based correlation spectra alone due to the occurrence of two molecules in the asymmetric unit cell of the sample. In addition, the unambiguous assignment of chemical shifts did not rely on comparison to those computed by DFT. In this instance, the enhanced sensitivity provided by MAS-DNP enabled 2D ^{13}C-^{13}C and ^{13}C-^{15}N through-space (dipolar) correlation experiments to be acquired. These dipolar-based experiments were necessary to obtain the atom connectivities because of the presence of interrupting nitrogen atoms in the deoxyguanosine ring structure, which prohibited the sole use of through-bond (*J*) correlation experiments.

4 – MAS-DNP-enabled NMR crystallography

^{13}C and ^{15}N spin dilution allows polarization transfer over long distance

The ability to use dipolar-based correlation experiments is important for probing proximities and thus to conduct resonance assignments (as explained above) but also raises the hope of accessing inter-nuclei distance information. Indeed, a mainstay of MAS ssNMR are the so-called dipolar recoupling experiments, where the dipolar coupling between nuclei, which is averaged by MAS, is reintroduced using dipolar recoupling pulse sequences. Because dipolar couplings are inversely proportional to the cube of the distance between the interacting nuclei, such experiments can be used to extract distance restraints. For instance, in the case of a doubly ^{13}C labeled compound, a precise distance estimate can be obtained between the spin-pair based on the characteristic time course of the polarization buildup.[11] However, the situation is more complicated in the case of uniformly (or densely) ^{13}C enriched samples, since a dense network of ^{13}C-^{13}C dipolar coupled nuclei is then created upon application of RF recoupling pulses. Such pulse sequences, called first-order recoupling sequences, are part of a large toolbox that includes HORROR/DREAM, DRAWS, POSTC7, SPC5, SR26, CMRR/CMAR, S3 etc.[58–67] One of the consequences of the

complex multi-spin dynamics is that the extraction of precise long distance information is becoming impossible because of a phenomenon called dipolar truncation.[11,68] This is illustrated in Figure 1a, which shows that polarization transfer to a distant nucleus (4.4 Å here) is strongly attenuated in the presence of a larger dipolar coupling, i.e. another nucleus at a shorter distance (1.5 Å). Such attenuation prevents the detection and the extraction of precise long distance information which would be valuable for structural studies.[68,69] As a result, 2D ^{13}C-^{13}C correlation experiments performed on uniformly ^{13}C labeled compounds (Figure 2) only contain cross-peaks that correspond to short distance correlations (one-bond transfer). Similar behavior can be expected for other densely coupled homonuclear networks, including ^{1}H-^{1}H spin systems under ultrafast-MAS.[70]

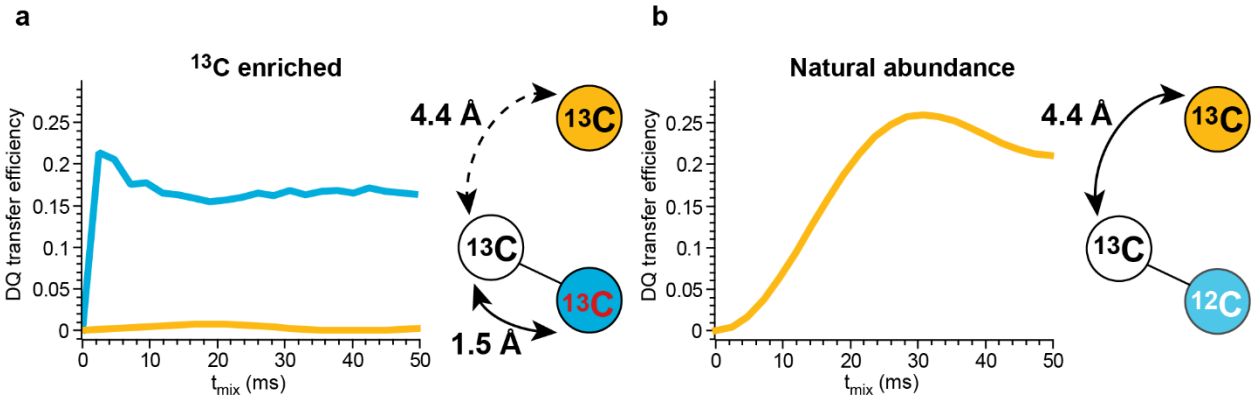

Figure 1. Simulated effects of dipolar truncation on double quantum (DQ) filtered ^{13}C-^{13}C recoupling. SPINEVOLUTION simulation of polarization transfer in a) a three-spin system, with two directly bonded ^{13}C spins (white and blue) at a 1.5 Å distance, and a third ^{13}C spin (yellow) 4.4 Å away. b) Only a 4.4 Å ^{13}C spin pair is considered, the third nucleus is ^{12}C. In a) efficient transfer is observed between the directly bonded ^{13}C spins (blue curve) whereas transfer to the third spin 4.4 Å away is attenuated (yellow curve) due to dipolar truncation. In contrast, in b) efficient transfer is observed for the lone 4.4 Å ^{13}C spin pair (yellow curve).

The dipolar truncation effect has long been a major bottleneck for structure determination of isotopically labeled biomolecular systems. As seen above, this effect is very intense for first-order homonuclear recoupling pulse sequences. It is however also present in heteronuclear cases if the dipolar recoupled terms do not commute with each other, like for instance in cross polarization (CP) based pulse sequences. This is not the case for REDOR and TEDOR heteronuclear recoupling sequences, which explains why these sequences were successfully used to extract precise distance

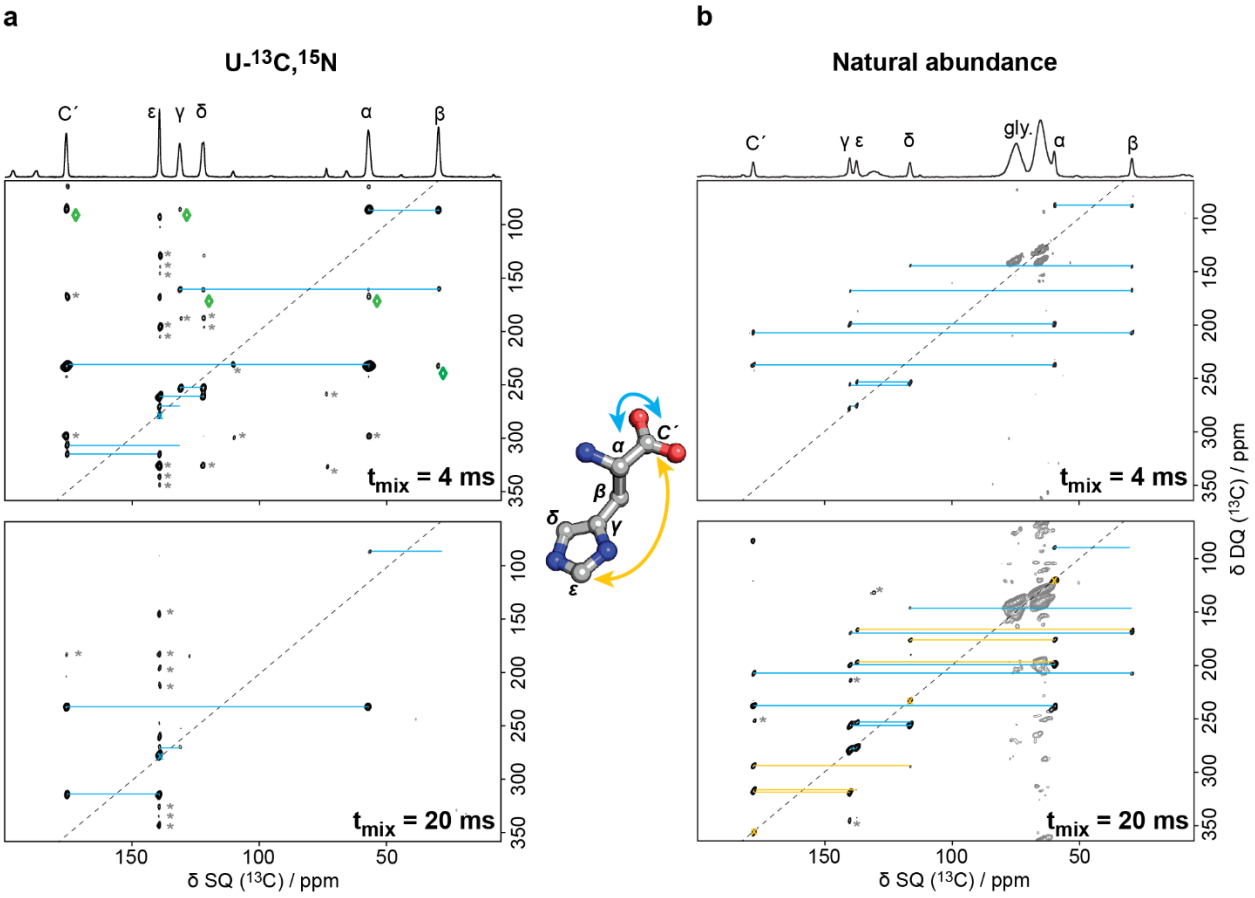

Figure 2. 2D DQ/SQ ^{13}C-^{13}C correlation spectra for a) uniformly ^{13}C,^{15}N-enriched and b) NA histidine. At NA, short-range correlations (blue lines) up to two bonds away are clearly observed with a 4 ms dipolar mixing time (top). At 20 ms (bottom) long-range (yellow lines) and short-range correlations are observed. At the same mixing times, only short-range correlations are observed in the U-^{13}C,^{15}N enriched histidine due to the effects of dipolar truncation. In addition,

in the U-^{13}C,^{15}N sample at the 4 ms mixing time the spectrum is complicated by the presence of correlations resulting from indirect transfers (green diamonds).[71] Asterisks mark spinning sidebands. The difference in assignment of the aromatic carbons is a result of different histidine tautomers between the two samples.[72] The spectra in b) were recorded using MAS-DNP.

information in ^{15}N/^{13}C labeled biomolecular systems. Still, even in these cases the presence of multiple spins complicates the analysis of experimental data, as shown for TEDOR experiments for example.[73]

To overcome the limitations described above, recoupling methods were developed with the goal to reduce dipolar truncation effects. Among them stand the Third Spin Assisted Recoupling (TSAR) methods, in which the polarization transfer between two spins X_1 and X_2 involves the couplings to an assisting nucleus, typically ^{1}H. More precisely, the associated pulse sequence relies on second-order cross-terms arising from ^{1}H-X_1 and ^{1}H-X_2 (where X = ^{13}C, ^{15}N, …) interactions.[65,74,75] The benefit of this approach is that long-distance correlations can be observed even in presence of strong dipolar couplings. However, it is important to stress that precise X_1-X_2 distance fitting remains challenging, principally because the polarization transfer does not directly depend upon the X_1-X_2 couplings, but rather upon the positioning of the surrounding ^{1}H spins.[69,75] Nevertheless, this approach can be used to estimate upper and/or lower bound distances and has been shown to provide very useful distance constraints for protein structure determination in ssNMR.[69,76]

The problem associated with dipolar truncation can be foiled by working with dilute spins, as is the case with ^{13}C and ^{15}N spins at their NA. For example, ^{13}C is 1.11 % abundant and as a result every particular ^{13}C-^{13}C spin pair is only 0.01 % abundant. Therefore, the probability of a ^{13}C-^{13}C spin-pair encountering a third perturbing ^{13}C nucleus that would contribute to dipolar truncation is

exceedingly low.[77–79] Because of this spin dilution effect at NA, first-order homonuclear dipolar recoupling sequences can now be used to detect long-distance polarization transfer once the sensitivity limitation is negated by the use of MAS-DNP.[78,79] This has been demonstrated in 2012 by Takahashi *et al.*,[79] and later used to detect both intra and intermolecular contacts in self-assembled peptides,[78] and to identify the correct polymorph of the pharmaceutical compound theophylline, as reported by Mollica et al., thanks to the use of dipolar buildups.[80]

Spin dilution grants access to precise long-range measurements

Later in 2017, Märker *et al.* presented the first detailed analysis of polarization buildup curves from ^{13}C-^{13}C dipolar recoupling experiments at NA.[77] It was shown that each buildup curve represents a superposition of buildup curves from several distance contributions, many of them being intermolecular, and that they are sensitive to distances up to ~7 Å. The simulation of spin pairs was sufficient to model these buildup curves and excellent agreement was obtained between the experimental buildup curves and simulated curves based on the crystal structure.

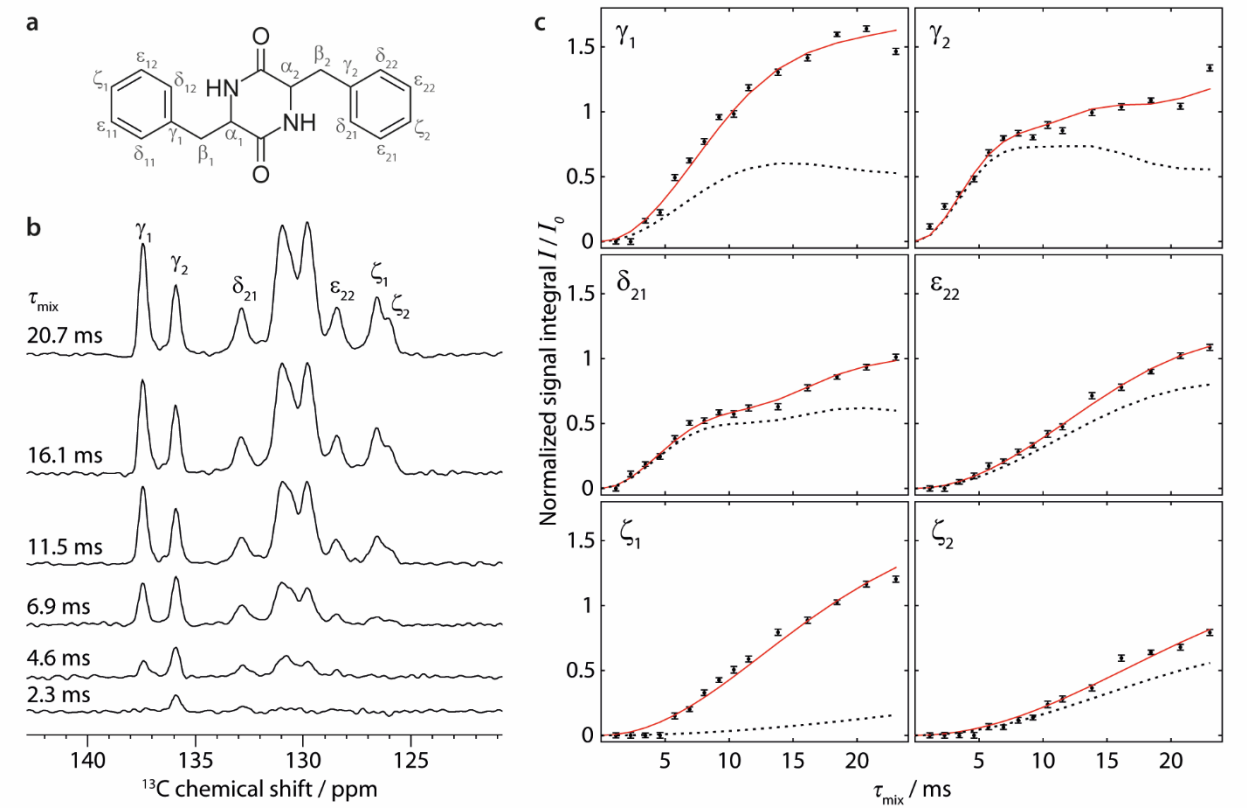

Figure 3. Molecular formula of cyclic diphenylalanine a) and buildup of aromatic resonances b) obtained after dipolar recoupling from selectively excited carbonyl resonances. c) Extracted experimental polarization buildup (black points) and numerical simulations of expected buildup curves based on the crystal structure, taking into account only intramolecular distances (black dashed lines) or all relevant distances up to 7 Å (red solid lines). Reprinted with permission from Märker *et al.* Copyright 2017, RSC (reference 73).

It is also possible to see several distances contribute to the same buildup curve when a given spin pair occurs at different distances. This can for instance be the case in a solid composed of small organic molecules where nucleus A can "see" nucleus B in the same molecule (intramolecular), but also in adjacent molecules (intermolecular). Therefore, experimental polarization buildup curves are often composed of a superposition of buildup curves corresponding to the different distances for a given spin-pair as illustrated in Figure 4. Multiple distances can in

principle be extracted from a given build up curve. However, an upper cutoff of the longest observable distance still exists, which is given by the efficiency of the dipolar recoupling sequence employed, but also by the probability of encountering a third truncating spin. This probability increases as the observation radius around the starting nucleus is increased and will eventually be 100 %, meaning that, statistically, no polarization transfer beyond this distance will be possible. This cutoff distance was estimated to lie between 7 and 8 Å in an organic solid with densely packed molecules.[77]

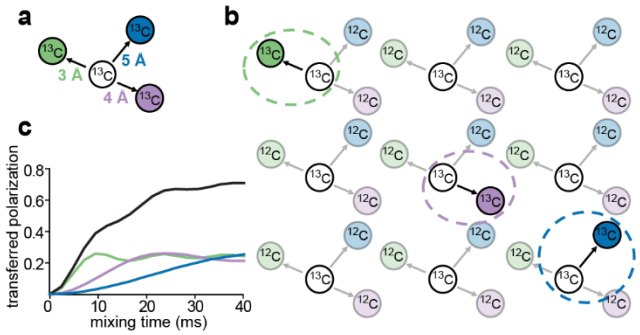

Figure 4. At NA only spin-pairs need to be considered for numerical simulation of polarization buildup curves. a) ^{13}C spin system with different distances between nuclei in an isotopically enriched spin system. b) The same spin system in a) is diluted at NA and only individual spin-pairs from the system are coupled. c) Characteristic buildup curves for ^{13}C-^{13}C spin-pairs at 3, 4, and 5 Å (green, purple, and blue curves respectively) and the resulting superposition of buildup curves for the three distances which can be expected for a sample at NA as in b).

Another benefit of recording polarization buildup curves at NA is that their analysis by numerical simulations (e.g. with SPINEVOLUTION, SIMPSON, etc…[81,82]) is considerably simplified compared to isotopically enriched samples. It is sufficient to consider only two interacting nuclei in each simulation and to sum up such spin-pair simulations as needed. This

results in very fast calculation times, especially compared to the more time-consuming simulation of multi-spin systems with various interacting nuclei and geometries.[81,83]

^{13}C spin dilution requires the use of DQ filtered experiments or selective spin flip.

While in general the same pulse sequences can be used with and without DNP, dipolar recoupling experiments between dilute nuclei pose special challenges. These arise because of the even lower abundance of the required spin pairs as most nuclei are not dipolar coupled to another nucleus of interest. Signals arising from spin pairs would therefore be buried under the much more intense signals originating from uncoupled spins. While this problem is naturally circumvented in heteronuclear correlation experiments, homonuclear correlations of dilute spins are greatly improved by using DQ filtration.[84,85] DQ-filtered experiments employ pulse sequences to create DQ coherences and exclusively select these coherences with a suitable phase cycle. As a DQ coherence can only be created between dipolar coupled spins, DQ filtration efficiently suppresses all signals from uncoupled spins. For such experiments, it should be kept in mind that the DQ filter removes half the signal, leading to a loss in sensitivity.[66]

Another way of suppressing the signal of uncoupled spins can be the use of selective pulses as demonstrated by Märker *et al.* for recoupling of ^{13}C nuclei at NA.[77] By selectively exciting a subset of resonances and subsequent application of a recoupling sequence, any signals building up on other resonances have to originate from the initially excited spin(s).[77] Such an experiment can be run without DQ filtration and collected as a series of 1D spectra, in contrast to the traditional approach that requires a set of 2D DQ/SQ correlation spectra to be recorded. This 1D method can therefore be very fast and attractive, but crucially depends on the applicability of selective pulses, i.e. it requires sufficient spectral dispersion of resonances.

When measuring long distances, i.e. small dipolar couplings, long recoupling times are required and the ideal recoupling sequence needs to be very robust with respect to interfering interactions such as chemical shift anisotropies and radio frequency pulse imperfections. Supercycled pulse sequences are usually best-suited for this purpose.[86] Efficient pulse sequences for homonuclear (DQ) recoupling are, for example, SR26 and S3,[59–61] whereas the *z*-filtered TEDOR sequence is a good option for heteronuclear recoupling.[73]

5 - Structural biology at NA

The structural characterization of biomolecules by ssNMR also benefits from experiments at NA, as long-range distance constraints again convey the most valuable structural information. Therefore, the reduced effects of dipolar truncation (discussed above) are also key in the characterization of biomolecules. An initial application of this approach was shown by Takahashi *et al.* where long-range correlations were observed for a self-assembled peptide and a globular protein using DQ/SQ ^{13}C-^{13}C correlation experiments at NA, enabled by MAS-DNP.[42,78] Previously, Zhou *et al*. showed that ^{13}C-^{1}H and ^{15}N-^{1}H correlation spectra of proteins could be obtained at NA, however, this was accomplished without MAS-DNP and therefore necessarily relied on the use of ^{1}H-detection schemes.[87]

In addition to avoiding the deleterious effects of dipolar truncation, it is also advantageous to study biomolecules at NA because it allows studying samples which are derived from sources that are difficult or impossible to isotopically enrich. One such example are amyloid fibrils, which are recognized for their role in numerous neurodegenerative diseases. It is known that the conditions under which protein monomers undergo aggregation can affect the conformation of the resulting fibril,[88–90] and it has been shown that different polymorphs can display varying levels of neurotoxicity.[91] Therefore, it is imperative to characterize the structure of protein aggregates that

are formed under native conditions. One route in achieving this goal is to study protein aggregates derived from patients or animal models, which necessitate that the aggregates are at NA. The prospects of this approach have been shown by Smith *et al.* who obtained ^{13}C-^{13}C DQ/SQ and ^{13}C-^{15}N correlation spectra for NA poly-glutamine (polyQ) fibrils which are the hallmark of Huntington's Disease.[92] These experiments demonstrated that a structural fingerprint, via ^{13}C and ^{15}N chemical shift assignment (Figure 5), of the amyloid core could be obtained at NA for protein fibrils. In addition, long-range distance restraints were obtained and aided in the characterization of the β-strand arrangement in the polyQ amyloid core. These types of measurements would not have been possible in uniformly ^{13}C enriched protein samples due to the effects of dipolar truncation.

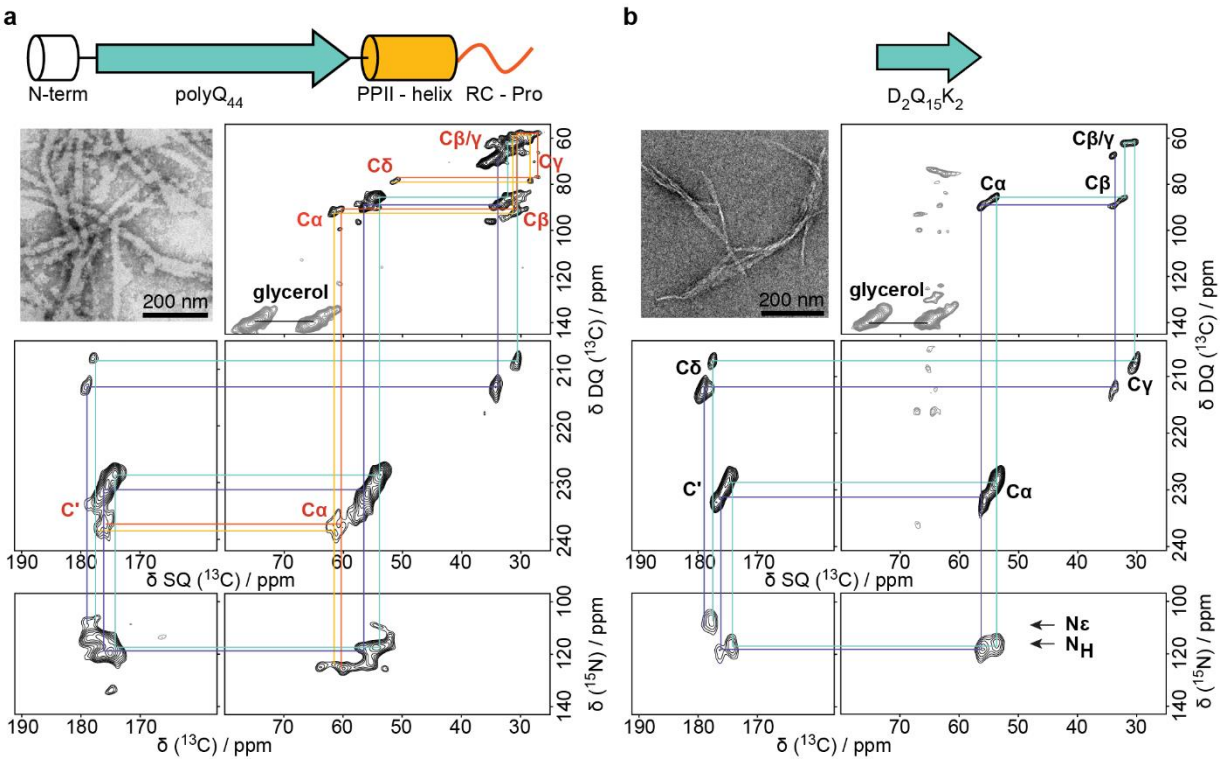

Figure 5. DQ/SQ ^{13}C-^{13}C and ^{13}C-^{15}N correlation spectra of a) mutant huntingtin protein fibrils with a 44-glutamine expansion and b) $D_2Q_{15}K_2$ peptide fibrils (model system for the polyQ amyloid core), both at NA. A short mixing time resulted in short-range ^{13}C-^{13}C and ^{13}C-^{15}N correlations and enabled assignment of the two types of glutamine in the polyQ amyloid core (purple and cyan) and the two oligoproline regions (orange and red). Reprinted with permission from Smith *et al.* Copyright 2018, American Chemical Society (reference 88).

Another example of the utility of NA studies of biomolecules was shown by Sinh S. *et al*.[93] who used MAS-DNP to investigate native bone collagen at NA. While collagen can be produced *in-vitro*, it is important to study it from native sources due to its numerous interactions with non-collagenous proteins that can impact its structure. In their study, CH/π interactions between the protons from the Cβ and Cγ of proline and hydroxyproline and the ring carbons of aromatic residues were observed via ^{1}H-^{13}C correlation experiments (Figure 6). Understanding these interactions is important because it is postulated that intermolecular interactions between aromatic residues and hydroxyproline and proline residues promote self-aggregation in collagen triple helices. These correlations are particularly difficult to observe if no MAS-DNP is employed due to the low occurrence (~ 1 %) of aromatic residues in collagen.

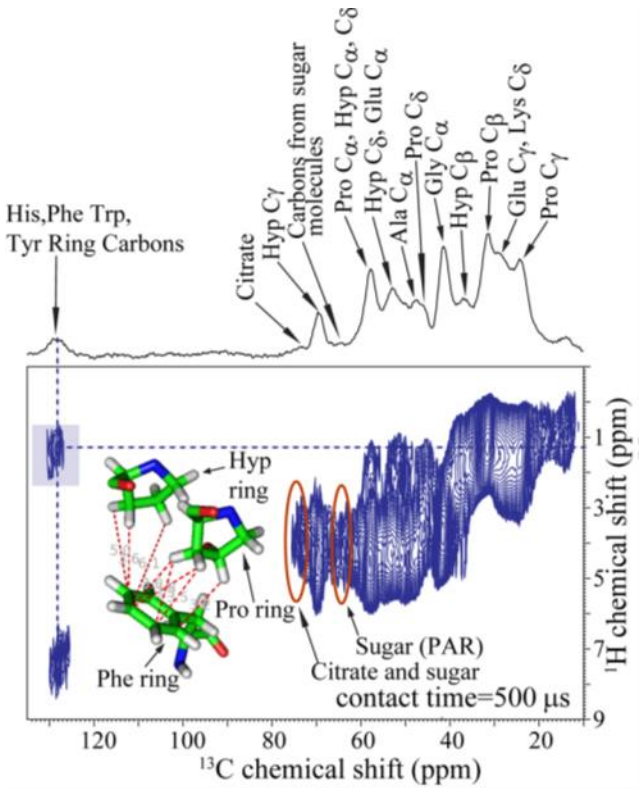

Figure 6. ^{1}H-^{13}C HETCOR spectrum of native collagen at NA. The highlighted cross peak (top left) denotes the correlation between ^{13}C from the rings of aromatic residues and ^{1}H's attached to the Cβ and Cγ of proline residues through CH/π interactions. Reprinted with permission from Singh *et al.* Copyright 2014, American Chemical Society (reference 89).

6 - Outlook

NA ssNMR experiments are challenging, however, with the impressive gains in sensitivity realized with MAS-DNP they are now achievable. Herein, we presented the advantages of NA ssNMR and some recent applications of the technique. Despite the significant progress made in this branch of MAS-DNP, there are still many advances to be made in the coming years, specifically, with further gains in MAS-DNP efficiency. Larger MAS-DNP enhancements will allow even more challenging samples to be studied and even more advanced/complicated NMR experiments to be performed at NA. Improvements in MAS-DNP efficiency will be ascertained

through concerted efforts primarily in hardware and polarization agent development and improved computational modeling.

A number of research groups are developing He based MAS instrumentation and have been able to perform MAS-DNP experiments at temperatures much lower than 100 K.[15,45,94–96] He MAS-DNP instrumentation is advantageous for numerous reasons, including, more favorable electron relaxation rates which should yield larger enhancements. Also, the fluid dynamic properties of He are better suited for fast MAS at similar temperatures compared to N_2 gas.[45,97] Currently, commercial MAS-DNP instrumentation uses N_2 for cooling and MAS, using He should allow rotors to be spun at rates comparable to conventional ssNMR (e.g. ~ 25 kHz for 3.2 mm rotors and ~ 60 kHz for 1.3 mm rotors). Faster MAS-DNP will expand the repertoire of pulse sequences that can be used at NA, for example, broadband dipolar recoupling sequences, and the use of low power or no ^{1}H decoupling.[11]

Improved polarization agents will also lead to more efficient MAS-DNP. Recently, a new class of nitroxide biradicals were introduced, the AsymPol family, which were designed with the aid of computational methods.[31] This represents a large step in the development of polarization agents that had solely relied on empirical evaluation in new radical design. The improved theoretical understanding of MAS-DNP mechanisms and the use of computational modeling of MAS-DNP processes will no doubt lead to further improvements in polarization agents. In addition to a new class of nitroxide biradicals, mixed biradicals also show promise for performing NA MAS-DNP at high-field (i.e. > 9.4 T). The combination of a narrow line radical (e.g. trityl or BDPA) and a wide line radical (e.g. nitroxide) have been used to perform DQ/SQ ^{13}C-^{13}C NA experiments on cellulose at 18.8 T (Figure 7); this was the first demonstration of NA MAS-DNP at high-field.[24] However, the latter experiment was completed in ~ 16 hours, whereas the same experiment only

took 20 minutes at 9.4 T (Figure 7). This clearly illustrates the need for further improvements in MAS-DNP efficiency, especially at high magnetic fields.

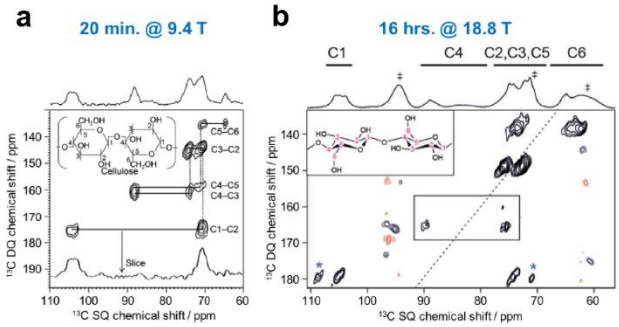

Figure 7. DQ/SQ ^{13}C-^{13}C correlation experiments at NA of cellulose at a) 9.4 T and b) 18.8 T. The experiment at 9.4 T was acquired in only 20 minutes, in contrast, it took ~ 16 hours at 18.8 T. Both samples were prepared with a minimum amount of glassy matrix in 3.2 mm rotors using TOTAPOL and TEMTriPol-1 polarizing agents in a) and b) respectively, additional details regarding the sample preparation can be found in the original publications. Reprinted with permission from Takahashi et al. Copyright 2012, Wiley-VCH (reference 75) and Mentink-Vigier et al. Copyright 2017, Royal Society of Chemistry (reference 20).

NA ssNMR enabled by MAS-DNP is opening up exciting new avenues for the characterization of both biomolecular samples and materials. It has aided in structural measurements of protein fibrils, self-assembled small molecules, pharmaceuticals, heterogeneous catalysts, and more. With further innovation NA ssNMR will no doubt continue to be a useful tool in the structural biology and materials chemistry communities.

AUTHOR INFORMATION

Notes

The authors declare no competing financial interests.

ACKNOWLEDGMENT

This work was funded by the European Union's Horizon 2020 research and innovation programme under the Marie Skłodowska-Curie Action-795423-BOLD-NMR (to A.N.S.) and the European Research Council grant ERC-CoG-2015 No. 682895 (to G.D.P). In addition, this work was partially supported by funding from the French National Research Agency (ANR-11-LABX-0003-01, ANR-15-IDEX-02, and ANR-16-CE11-0030).

REFERENCES

(1) Renault, M.; Cukkemane, A.; Baldus, M. Solid-State NMR Spectroscopy on Complex Biomolecules. *Angew. Chemie - Int. Ed.* **2010**, *49* (45), 8346–8357.

(2) Bryce, D. L. NMR Crystallography: Structure and Properties of Materials from Solid-State Nuclear Magnetic Resonance Observables. *IUCrJ* **2017**, *4*, 350–359.

(3) Harris, R. K. Applications of Solid-State NMR to Pharmaceutical Polymorphism and Related Matters*. *J. Pharm. Pharmacol.* **2007**, *59* (2), 225–239.

(4) Zhang, W.; Xu, S.; Han, X.; Bao, X. In Situ Solid-State NMR for Heterogeneous Catalysis: A Joint Experimental and Theoretical Approach. *Chem. Soc. Rev.* **2012**, *41* (1), 192–210.

(5) Kovacs, H.; Moskau, D.; Spraul, M. Cryogenically Cooled Probes - A Leap in NMR Technology. *Prog. Nucl. Magn. Reson. Spectrosc.* **2005**, *46* (2-3), 131–155.

(6) Hong, M.; Jakes, K. Selective and Extensive ^{13}C Labeling of a Membrane Protein for Solid- State NMR Investigations. *J. Biomol. NMR* **1999**, *14* (1), 71–74.

(7) Kwon, B.; Tietze, D.; White, P. B.; Liao, S. Y.; Hong, M. Chemical Ligation of the Influenza M2 Protein for Solid-State NMR Characterization of the Cytoplasmic Domain. *Protein Sci.* **2015**, *24* (7), 1087–1099.

(8) Higman, V. A.; Flinders, J.; Hiller, M.; Jehle, S.; Markovic, S.; Fiedler, S.; van Rossum, B.-J.; Oschkinat, H. Assigning Large Proteins in the Solid State: A MAS NMR Resonance

Assignment Strategy Using Selectively and Extensively ^{13}C-Labelled Proteins. *J. Biomol. NMR* **2009**, *44* (4), 245–260.

(9) Loquet, A.; Lv, G.; Giller, K.; Becker, S.; Lange, A. ^{13}C Spin Dilution for Simplified and Complete Solid-State NMR Resonance Assignment of Insoluble Biological Assemblies. *J. Am. Chem. Soc.* **2011**, *133* (13), 4722–4725.

(10) Skrisovska, L.; Schubert, M.; Allain, F. H. T. Recent Advances in Segmental Isotope Labeling of Proteins: NMR Applications to Large Proteins and Glycoproteins. *J. Biomol. NMR* **2010**, *46* (1), 51–65.

(11) De Paëpe, G. Dipolar Recoupling in Magic Angle Spinning Solid-State Nuclear Magnetic Resonance. *Annu. Rev. Phys. Chem.* **2012**, *63* (1), 661–684.

(12) Fu, R.; Brey, W. W.; Shetty, K.; Gor'kov, P.; Saha, S.; Long, J. R.; Grant, S. C.; Chekmenev, E. Y.; Hu, J.; Gan, Z.; et al. Ultra-Wide Bore 900 MHz High-Resolution NMR at the National High Magnetic Field Laboratory. *J. Magn. Reson.* **2005**, *177* (1), 1–8.

(13) Gan, Z.; Hung, I.; Wang, X.; Paulino, J.; Wu, G.; Litvak, I. M.; Gor'kov, P. L.; Brey, W. W.; Lendi, P.; Schiano, J. L.; et al. NMR Spectroscopy up to 35.2 T Using a Series-Connected Hybrid Magnet. *J. Magn. Reson.* **2017**, *284*, 125–136.

(14) Becerra, L. R.; Gerfen, G. J.; Temkin, R. J.; Singel, D. J.; Griffin, R. G. Dynamic Nuclear Polarization with a Cyclotron Resonance Maser at 5 T. *Phys. Rev. Lett.* **1993**, *71* (21), 3561–3564.

(15) Hall, D. A.; Maus, D. C.; Gerfen, G. J.; Inati, S. J.; Becerra, L. R.; Dahlquist, F. W.; Griffin, R. G. Polarization-Enhanced NMR Spectroscopy of Biomolecules in Frozen Solution. *Science (80-.).* **1997**, *276* (5314), 930–932.

(16) Smith, A. N.; Long, J. R. Dynamic Nuclear Polarization as an Enabling Technology for Solid State Nuclear Magnetic Resonance Spectroscopy. *Anal. Chem.* **2016**, *88* (1), 122–132.

(17) Lee, D.; Hediger, S.; De Paëpe, G. Is Solid-State NMR Enhanced by Dynamic Nuclear Polarization? *Solid State Nucl. Magn. Reson.* **2015**, *66*, 6–20.

(18) Blanc, F.; Sperrin, L.; Jefferson, D. A.; Pawsey, S.; Rosay, M.; Grey, C. P. Dynamic Nuclear Polarization Enhanced Natural abundance ^{17}O Spectroscopy. *J. Am. Chem. Soc.* **2013**, *135* (8), 2975–2978.

(19) Blanc, F.; Sperrin, L.; Lee, D.; Dervişoğlu, R.; Yamazaki, Y.; Haile, S. M.; De Paëpe, G.; Grey, C. P. Dynamic Nuclear Polarization NMR of Low-γ Nuclei: Structural Insights into Hydrated Yttrium-Doped $BaZrO_3$. *J. Phys. Chem. Lett.* **2014**, *5* (14), 2431–2436.

(20) Perras, F.A.; Padmos, J. D.; Johnson, R. L.; Wang, L. L.; Schwartz, T. J.; Kobayashi, T.; Horton, J. H.; Dumesic, J. A.; Shanks, B. H.; Johnson, D. D.; et al. Characterizing Substrate-Surface Interactions on Alumina-Supported Metal Catalysts by Dynamic Nuclear Polarization-Enhanced Double-Resonance NMR Spectroscopy. *J. Am. Chem. Soc.* **2017**, *139* (7), 2702–2709.

(21) Lee, D.; Leroy, C.; Crevant, C.; Bonhomme-Coury, L.; Babonneau, F.; Laurencin, D.; Bonhomme, C.; De Paëpe, G. Interfacial Ca2+ Environments in Nanocrystalline Apatites Revealed by Dynamic Nuclear Polarization Enhanced ^{43}Ca NMR Spectroscopy. *Nat. Commun.* **2017**, *8*, 14104.

(22) Overhauser, A. W. Polarization of Nuclei in Metals. *Phys. Rev.* **1953**, *92* (2), 411–415.

(23) Carver, T. R.; Slichter, C. P. Polarization of Nuclear Spins in Metals [15]. *Phys. Rev.* **1953**, *92* (1), 212–213.

(24) Mentink-Vigier, F.; Mathies, G.; Liu, Y.; Barra, A. L.; Caporini, M. A.; Lee, D.; Hediger, S.; Griffin, R.; De Paëpe, G. Efficient Cross-Effect Dynamic Nuclear Polarization without Depolarization in High-Resolution MAS NMR. *Chem. Sci.* **2017**, *8* (12), 8150–8163.

(25) Thurber, K. R.; Tycko, R. Theory for Cross Effect Dynamic Nuclear Polarization under Magic-Angle Spinning in Solid State Nuclear Magnetic Resonance: The Importance of Level Crossings. *J. Chem. Phys.* **2012**, *137* (8).

(26) Mentink-Vigier, F.; Akbey, Ü.; Hovav, Y.; Vega, S.; Oschkinat, H.; Feintuch, A. Fast Passage Dynamic Nuclear Polarization on Rotating Solids. *J. Magn. Reson.* **2012**, *224*, 13–21.

(27) Thurber, K. R.; Tycko, R. Perturbation of Nuclear Spin Polarizations in Solid State NMR of Nitroxide-Doped Samples by Magic-Angle Spinning without Microwaves. *J. Chem. Phys.* **2014**, *140* (18).

(28) Mentink-Vigier, F.; Paul, S.; Lee, D.; Feintuch, A.; Hediger, S.; Vega, S.; De Paëpe, G. Nuclear Depolarization and Absolute Sensitivity in Magic-Angle Spinning Cross-Effect Dynamic Nuclear Polarization. *Phys. Chem. Chem. Phys.* **2015**, -.

(29) Song, C.; Hu, K. N.; Joo, C. G.; Swager, T. M.; Griffin, R. G. TOTAPOL: A Biradical Polarizing Agent for Dynamic Nuclear Polarization Experiments in Aqueous Media. *J. Am. Chem. Soc.* **2006**, *128* (35), 11385–11390.

(30) Hu, K. N.; Song, C.; Yu, H. H.; Swager, T. M.; Griffin, R. G. High-Frequency Dynamic Nuclear Polarization Using Biradicals: A Multifrequency EPR Lineshape Analysis. *J. Chem. Phys.* **2008**, *128* (5).

(31) Mentink-Vigier, F.; Marin-Montesinos, I.; Jagtap, A. P.; Halbritter, T.; Van Tol, J.; Hediger, S.; Lee, D.; Sigurdsson, S. T.; De Paëpe, G. Computationally-Assisted Design of

Polarizing Agents for Dynamic Nuclear Polarization Enhanced NMR: The AsymPol Family. *J. Am. Chem. Soc.* **2018**, jacs.8b04911.

(32) Van der Cruijsen, E. A. W.; Koers, E. J.; Sauvée, C.; Hulse, R. E.; Weingarth, M.; Ouari, O.; Perozo, E.; Tordo, P.; Baldus, M. Biomolecular DNP-Supported NMR Spectroscopy Using Site-Directed Spin Labeling. *Chem. - A Eur. J.* **2015**, *21* (37), 12971–12977.

(33) Voinov, M. A.; Good, D. B.; Ward, M. E.; Milikisiyants, S.; Marek, A.; Caporini, M. a.; Rosay, M.; Munro, R. A.; Ljumovic, M.; Brown, L. S.; et al. Cysteine-Specific Labeling of Proteins with a Nitroxide Biradical for Dynamic Nuclear Polarization NMR. *J. Phys. Chem. B* **2015**, *119* (32), 10180–10190.

(34) Salnikov, E. S.; Abel, S.; Karthikeyan, G.; Karoui, H.; Aussenac, F.; Tordo, P.; Bechinger, B.; Ouari, O. Dynamic Nuclear Polarization/Solid-State NMR Spectroscopy of Membrane Polypeptides: Free-Radical Optimization for Matrix-Free Lipid Bilayer Samples. *ChemPhysChem* **2017**, *18* (15), 2103–2113.

(35) Rogawski, R.; Sergeyev, I. V.; Li, Y.; Ottaviani, M. F.; Cornish, V.; McDermott, A. E. Dynamic Nuclear Polarization Signal Enhancement with High-Affinity Biradical Tags. *J. Phys. Chem. B* **2017**, *121* (6), 1169–1175.

(36) Smith, A. N.; Caporini, M. A.; Fanucci, G. E.; Long, J. R. A Method for Dynamic Nuclear Polarization Enhancement of Membrane Proteins. *Angew. Chemie - Int. Ed.* **2015**, *54* (5), 1542–1546.

(37) Smith, A. N.; Twahir, U. T.; Dubroca, T.; Fanucci, G. E.; Long, J. R. Molecular Rationale for Improved Dynamic Nuclear Polarization of Biomembranes. *J. Phys. Chem. B* **2016**, *120* (32), 7880–7888.

(38) Fernández-de-Alba, C.; Takahashi, H.; Richard, A.; Chenavier, Y.; Dubois, L.; Maurel, V.; Lee, D.; Hediger, S.; De Paëpe, G. Matrix-Free DNP-Enhanced NMR Spectroscopy of Liposomes Using a Lipid-Anchored Biradical. *Chem. - A Eur. J.* **2015**, *21* (12), 4512–4517.

(39) Albert, B. J.; Gao, C.; Sesti, E. L.; Saliba, E. P.; Alaniva, N.; Scott, F. J.; Sigurdsson, S. T.; Barnes, A. B. Dynamic Nuclear Polarization Nuclear Magnetic Resonance in Human Cells Using Fluorescent Polarizing Agents. *Biochemistry* **2018**, *57* (31), 4741–4746.

(40) Takahashi, H.; Ayala, I.; Bardet, M.; De Paëpe, G.; Simorre, J. P.; Hediger, S. Solid-State NMR on Bacterial Cells: Selective Cell Wall Signal Enhancement and Resolution Improvement Using Dynamic Nuclear Polarization. *J. Am. Chem. Soc.* **2013**, *135* (13), 5105–5110.

(41) Lesage, A.; Lelli, M.; Gajan, D.; Caporini, M. A.; Vitzthum, V.; Miéville, P.; Alauzun, J.; Roussey, A.; Thieuleux, C.; Mehdi, A.; et al. Surface Enhanced NMR Spectroscopy by Dynamic Nuclear Polarization. *J. Am. Chem. Soc.* **2010**, *132* (44), 15459–15461.

(42) Takahashi, H.; Hediger, S.; De Paëpe, G. Matrix-Free Dynamic Nuclear Polarization Enables Solid-State NMR ^{13}C–^{13}C Correlation Spectroscopy of Proteins at Natural Isotopic Abundance. *Chem. Commun.* **2013**, *49* (82), 9479.

(43) Le, D.; Casano, G.; Phan, T. N. T.; Ziarelli, F.; Ouari, O.; Aussenac, F.; Thureau, P.; Mollica, G.; Gigmes, D.; Tordo, P. Optimizing Sample Preparation Methods for Dynamic Nuclear Polarization Solid-State NMR of Synthetic Polymers. **2014**.

(44) Rosay, M.; Blank, M.; Engelke, F. Instrumentation for Solid-State Dynamic Nuclear Polarization with Magic Angle Spinning NMR. *J. Magn. Reson.* **2016**, *264*, 88–98.

(45) Bouleau, E.; Saint-Bonnet, P.; Mentink-Vigier, F.; Takahashi, H.; Jacquot, J. F.; Bardet, M.; Aussenac, F.; Purea, A.; Engelke, F.; Hediger, S.; et al. Pushing NMR Sensitivity Limits Using Dynamic Nuclear Polarization with Closed-Loop Cryogenic Helium Sample Spinning. *Chem. Sci.* **2015**, *6* (12), 6806–6812.

(46) Thurber, K. R.; Potapov, A.; Yau, W. M.; Tycko, R. Solid State Nuclear Magnetic Resonance with Magic-Angle Spinning and Dynamic Nuclear Polarization below 25 K. *J. Magn. Reson.* **2013**, *226*, 100–106.

(47) Baias, M.; Dumez, J. N.; Svensson, P. H.; Schantz, S.; Day, G. M.; Emsley, L. De Novo Determination of the Crystal Structure of a Large Drug Molecule by Crystal Structure Prediction-Based Powder NMR Crystallography. *J. Am. Chem. Soc.* **2013**, *135* (46), 17501–17507.

(48) Salager, E.; Day, G. M.; Stein, R. S.; Pickard, C. J.; Elena, B.; Emsley, L. Powder Crystallography by Combined Crystal Structure Prediction and High-resolution ^{1}H Solid-State NMR Spectroscopy. *J. Am. Chem. Soc.* **2010**, *132* (8), 2564–2566.

(49) Paruzzo, F. M.; Hofstetter, A.; Musil, F.; De, S.; Ceriotti, M.; Emsley, L. Chemical Shifts in Molecular Solids by Machine Learning. *Nat. Commun.* **2018**, *9*, 4501.

(50) Lesage, A.; Auger, C.; Caldarelli, S.; Emsley, L. Determination of through-Bond Carbon-Carbon Connectivities in Solid-State NMR Using the INADEAUATE Experiment. *J. Am. Chem. Soc.* **1997**, *119* (33), 7867–7868.

(51) Lesage, A.; Bardet, M.; Emsley, L. Through-Bond Carbon-Carbon Connectivities in Disordered Solids by NMR. *J. Am. Chem. Soc.* **1999**, *121* (47), 10987–10993.

(52) Andreas, L. B.; Jaudzems, K.; Stanek, J.; Lalli, D.; Bertarello, A.; Le Marchand, T.; Cala-De Paepe, D.; Kotelovica, S.; Akopjana, I.; Knott, B.; et al. Structure of Fully Protonated Proteins by Proton-Detected Magic-Angle Spinning NMR. *Proc. Natl. Acad. Sci.* **2016**, *113* (33), 9187–9192.

(53) Rossini, A. J.; Zagdoun, A.; Lelli, M.; Lesage, A.; Copéret, C.; Emsley, L. Dynamic Nuclear Polarization Surface Enhanced NMR Spectroscopy. *Acc. Chem. Res.* **2013**, *46* (9), 1942–1951.

(54) Rossini, A. J.; Widdifield, C. M.; Zagdoun, A.; Lelli, M.; Schwarzwälder, M.; Copéret, C.; Lesage, A.; Emsley, L. Dynamic Nuclear Polarization Enhanced NMR Spectroscopy for Pharmaceutical Formulations. *J. Am. Chem. Soc.* **2014**, *136* (6), 2324–2334.

(55) Ni, Q. Z.; Yang, F.; Can, T. V.; Sergeyev, I. V.; D'Addio, S. M.; Jawla, S. K.; Li, Y.; Lipert, M. P.; Xu, W.; Williamson, R. T.; et al. In-Situ Characterization of Pharmaceutical Formulations by Dynamic Nuclear Polarization Enhanced MAS NMR. *J. Phys. Chem. B* **2017**, acs.jpcb.7b07213.

(56) Pinon, A. C.; Rossini, A. J.; Widdifield, C. M.; Gajan, D.; Emsley, L. Polymorphs of Theophylline Characterized by DNP Enhanced Solid-State NMR. *Mol. Pharm.* **2015**, *12* (11), 4146–4153.

(57) Märker, K.; Pingret, M.; Mouesca, J. M.; Gasparutto, D.; Hediger, S.; De Paëpe, G. A New Tool for NMR Crystallography: Complete 13C/15N Assignment of Organic Molecules at Natural Isotopic Abundance Using DNP-Enhanced Solid-State NMR. *J. Am. Chem. Soc.* **2015**, *137* (43), 13796–13799.

(58) Hohwy, M.; Jakobsen, H. J.; Edén, M.; Levitt, M. H.; Nielsen, N. C. Broadband Dipolar Recoupling in the Nuclear Magnetic Resonance of Rotating Solids: A Compensated C7 Pulse Sequence. *J. Chem. Phys.* **1998**, *108* (7), 2686–2694.

(59) Kristiansen, P. E.; Carravetta, M.; Lai, W. C.; Levitt, M. H. A Robust Pulse Sequence for the Determination of Small Homonuclear Dipolar Couplings in Magic-Angle Spinning NMR. *Chem. Phys. Lett.* **2004**, *390* (1-3), 1–7.

(60) Teymoori, G.; Pahari, B.; Stevensson, B.; Edén, M. Low-Power Broadband Homonuclear Dipolar Recoupling without Decoupling: Double-quantum13C NMR Correlations at Very Fast Magic-Angle Spinning. *Chem. Phys. Lett.* **2012**, *547*, 103–109.

(61) Teymoori, G.; Pahari, B.; Edén, M. Low-Power Broadband Homonuclear Dipolar Recoupling in MAS NMR by Two-Fold Symmetry Pulse Schemes for Magnetization Transfers and Double-Quantum Excitation. *J. Magn. Reson.* **2015**, *261*, 205–220.

(62) Gregory, D. M.; Mitchell, D. J.; Stringer, J. A.; Kiihne, S.; Shiels, J. C.; Callahan, J.; Mehta, M. A.; Drobny, G. P. Windowless Dipolar Recoupling: The Detection of Weak Dipolar Couplings between Spin 1 2 Nuclei with Large Chemical Shift Anisotropies. *Chem. Phys. Lett.* **1995**, *246* (6), 654–663.

(63) Hohwy, M.; Rienstra, C. M.; Jaroniec, C. P.; Griffin, R. G. Fivefold Symmetric Homonuclear Dipolar Recoupling in Rotating Solids: Application to Double Quantum Spectroscopy. *J. Chem. Phys.* **1999**, *110* (16), 7983–7992.

(64) De Paëpe, G.; Bayro, M. J.; Lewandowski, J.; Griffin, R. G. Broadband Homonuclear Correlation Spectroscopy at High Magnetic Fields and MAS Frequencies. *J. Am. Chem. Soc.* **2006**, *128* (6), 1776–1777.

(65) De Paëpe, G.; Lewandowski, J. R.; Griffin, R. G. Spin Dynamics in the Modulation Frame: Application to Homonuclear Recoupling in Magic Angle Spinning Solid-State NMR. *J. Chem. Phys.* **2008**, *128* (12), 124503.

(66) Nielsen, N. C.; Bildsøe, H.; Jakobsen, H. J.; Levitt, M. H. Double-Quantum Homonuclear Rotary Resonance: Efficient Dipolar Recovery in Magic-Angle Spinning Nuclear Magnetic Resonance. *J. Chem. Phys.* **1994**, *101* (3), 1805–1812.

(67) Verel, R.; Baldus, M.; Ernst, M.; Meier, B. H. A Homonuclear Spin-Pair Filter for Solid-State NMR Based on Adiabatic-Passage Techniques. *Chem. Phys. Lett.* **1998**, *287* (3-4), 421–428.

(68) Costa, P. R. Spins, Peptides, and Alzheimer's Disease: Solid-State Nuclear Magnetic Resonance Investigations of Amyloid Peptide Conformation. Massachusetts Institute of Technology PhD. Dissertation. **1996**.

(69) De Paëpe, G.; Lewandowski, J. R.; Loquet, A.; Böckmann, A.; Griffin, R. G. Proton Assisted Recoupling and Protein Structure Determination. *J. Chem. Phys.* **2008**, *129* (24).

(70) Xue, K.; Sarkar, R.; Motz, C.; Asami, S.; Camargo, D. C. R.; Decker, V.; Wegner, S.; Tosner, Z.; Reif, B. Limits of Resolution and Sensitivity of Proton Detected MAS Solid-State NMR Experiments at 111 kHz in Deuterated and Protonated Proteins. *Sci. Rep.* **2017**, *7* (1), 1–7.

(71) Brinkmann, A.; Edén, M.; Levitt, M. H. Synchronous Helical Pulse Sequences in Magic-Angle Spinning Nuclear Magnetic Resonance: Double Quantum Recoupling of Multiple-Spin Systems. *J. Chem. Phys.* **2000**, *112* (19), 8539–8554.

(72) Sudmeier, J. L.; Bradshaw, E. M.; Coffman Haddad, K. E.; Day, R. M.; Thalhauser, C. J.; Bullock, P. a.; Bachovchin, W. W. Identification of Histidine Tautomers in Proteins by 2D 1H/13Cδ2 One-Bond Correlated NMR. *J. Am. Chem. Soc.* **2003**, *125* (28), 8430–8431.

(73) Jaroniec, C. P.; Filip, C.; Griffin, R. G. 3D TEDOR NMR Experiments for the Simultaneous Measurement of Multiple Carbon-Nitrogen Distances in Uniformly 13C,15N-Labeled Solids. *J. Am. Chem. Soc.* **2002**, *124* (36), 10728–10742.

(74) Lewandowski, J. R.; De Paëpe, G.; Griffin, R. G. Proton Assisted Insensitive Nuclei Cross Polarization. *J. Am. Chem. Soc.* **2007**, *129* (4), 728–729.

(75) Paëpe, G. De; Lewandowski, J. R.; Loquet, A.; Eddy, M.; Megy, S.; Böckmann, A.; Griffin, R. G. Heteronuclear Proton Assisted Recoupling. *J. Chem. Phys.* **2011**, *134* (9).

(76) Bertini, I.; Bhaumik, A.; Griffin, R. G.; Lelli, M.; Lewandowski, R.; Luchinat, C. High-Resolution Solid-State NMR Structure of a 17 . 6 kDa Protein. **2010**, No. 22, 1032–1040.

(77) Märker, K.; Paul, S.; Fernández-de-Alba, C.; Lee, D.; Mouesca, J.-M.; Hediger, S.; De Paëpe, G. Welcoming Natural Isotopic Abundance in Solid-State NMR: Probing Π-Stacking and Supramolecular Structure of Organic Nanoassemblies Using DNP. *Chem. Sci.* **2017**, *8* (2), 974–987.

(78) Takahashi, H.; Viverge, B.; Lee, D.; Rannou, P.; De Paëpe, G. Towards Structure Determination of Self-Assembled Peptides Using Dynamic Nuclear Polarization Enhanced Solid-State NMR Spectroscopy. *Angew. Chemie - Int. Ed.* **2013**, *52* (27), 6979–6982.

(79) Takahashi, H.; Lee, D.; Dubois, L.; Bardet, M.; Hediger, S.; Depaëpe, G. Rapid Natural-Abundance 2D ^{13}C-^{13}C Correlation Spectroscopy Using Dynamic Nuclear Polarization Enhanced Solid-State NMR and Matrix-Free Sample Preparation. *Angew. Chemie - Int. Ed.* **2012**, *51* (47), 11766–11769.

(80) Mollica, G.; Dekhil, M.; Ziarelli, F.; Thureau, P.; Viel, S. Quantitative Structural Constraints for Organic Powders at Natural Isotopic Abundance Using Dynamic Nuclear Polarization Solid-State NMR Spectroscopy. *Angew. Chemie - Int. Ed.* **2015**, *54* (20), 6028–6031.

(81) Veshtort, M.; Griffin, R. G. SPINEVOLUTION: A Powerful Tool for the Simulation of Solid and Liquid State NMR Experiments. *J. Magn. Reson.* **2006**, *178* (2), 248–282.

(82) Bak, M.; Rasmussen, J. T.; Nielsen, N. C. SIMPSON: A General Simulation Program for Solid-State NMR Spectroscopy. *J. Magn. Reson.* **2000**, *147* (2), 296–330.

(83) Tošner, Z.; Andersen, R.; Stevensson, B.; Edén, M.; Nielsen, N. C.; Vosegaard, T. Computer-Intensive Simulation of Solid-State NMR Experiments Using SIMPSON. *J. Magn. Reson.* **2014**, *246*, 79–93.

(84) Wokaun, A.; Ernst, R. R. Selective Detection of Multiple Quantum Transitions in NMR. *Chem. Phys. Lett.* **1977**, *52* (3), 407–412.

(85) Bax, A.; Freeman, R.; Frenkiel, T. A. An NMR Technique for Tracing Out the Carbon Skeleton of an Organic Molecule. *J. Am. Chem. Soc.* **1981**, *103* (8), 2102–2104.

(86) Kristiansen, P. E.; Carravetta, M.; Van Beek, J. D.; Lai, W. C.; Levitt, M. H. Theory and Applications of Supercycled Symmetry-Based Recoupling Sequences in Solid-State Nuclear Magnetic Resonance. *J. Chem. Phys.* **2006**, *124* (23).

(87) Zhou, D. H.; Shah, G.; Mullen, C.; Sandoz, D.; Rienstra, C. M. Proton-Detected Solid-State NMR Spectroscopy of Natural-Abundance Peptide and Protein Pharmaceuticals. *Angew. Chemie - Int. Ed.* **2009**, *48* (7), 1253–1256.

(88) Van Der Wel, P. C. A. Insights into Protein Misfolding and Aggregation Enabled by Solid-State NMR Spectroscopy. *Solid State Nucl. Magn. Reson.* **2017**, *88* (October), 1–14.

(89) Tycko, R. Amyloid Polymorphism: Structural Basis and Neurobiological Relevance. *Neuron* **2015**, *86* (3), 632–645.

(90) Frederick, K. K.; Michaelis, V. K.; Corzilius, B.; Ong, T. C.; Jacavone, A. C.; Griffin, R. G.; Lindquist, S. Sensitivity-Enhanced NMR Reveals Alterations in Protein Structure by Cellular Milieus. *Cell* **2015**, *163* (3), 620–628.

(91) Lin, H.-K.; Boatz, J. C.; Krabbendam, I. E.; Kodali, R.; Hou, Z.; Wetzel, R.; Dolga, A. M.; Poirier, M. A.; van der Wel, P. C. a. Fibril Polymorphism Affects Immobilized Non-Amyloid Flanking Domains of Huntingtin exon1 rather than Its Polyglutamine Core. *Nat. Commun.* **2017**, *8* (May), 15462.

(92) Smith, A. N.; Märker, K.; Piretra, T.; Boatz, J. C.; Matlahov, I.; Kodali, R.; Hediger, S.; Van Der Wel, P. C. A.; De Paëpe, G. Structural Fingerprinting of Protein Aggregates by Dynamic Nuclear Polarization-Enhanced Solid-State NMR at Natural Isotopic Abundance. *J. Am. Chem. Soc.* **2018**, *140* (44), 14576–14580.

(93) Singh, C.; Rai, R. K.; Aussenac, F.; Sinha, N. Direct Evidence of Imino Acid-Aromatic Interactions in Native Collagen Protein by DNP-Enhanced Solid-State NMR Spectroscopy. *J. Phys. Chem. Lett.* **2014**, *5* (22), 4044–4048.

(94) Thurber, K.; Tycko, R. Low-Temperature Dynamic Nuclear Polarization with Helium-Cooled Samples and Nitrogen-Driven Magic-Angle Spinning. *J. Magn. Reson.* **2016**, *264*, 99–106.

(95) Sesti, E. L.; Saliba, E. P.; Alaniva, N.; Barnes, A. B. Electron Decoupling with Cross Polarization and Dynamic Nuclear Polarization below 6 K. *J. Magn. Reson.* **2018**, *295*, 1–5.

(96) Matsuki, Y.; Ueda, K.; Idehara, T.; Ikeda, R.; Ogawa, I.; Nakamura, S. Helium-Cooling and -Spinning Dynamic Nuclear Polarization for Sensitivity-Enhanced Solid-State NMR at 14 T and 30 K. *J. Magn. Reson.* **2012**, *225*, 1–9.

(97) Lee, D.; Bouleau, E.; Saint-Bonnet, P.; Hediger, S.; De Paëpe, G. Ultra-Low Temperature MAS-DNP. *J. Magn. Reson.* **2016**, *264*, 116–124.